# Optical Lithography

## Here Is Why SECOND EDITION

Burn J. Lin

**SPIE PRESS**
Bellingham, Washington USA

Library of Congress Cataloging-in-Publication Data

Names: Lin, Burn Jeng, 1942– author.
Title: Optical lithography : here is why / Burn J. Lin.
Description: Second edition. | Bellingham, Washington : SPIE, [2021] | Includes bibliographical references and index.
Identifiers: LCCN 2020049077 (print) | LCCN 2020049078 (ebook) | ISBN 9781510639959 (hardcover) | ISBN 9781510639966 (pdf)
Subjects: LCSH: Microlithography. | Semiconductors–Etching. | Lasers–Industrial applications.
Classification: LCC TK7872.M3 .L56 2021 (print) | LCC TK7872.M3 (ebook) | DDC 621.3815/31–dc22
LC record available at https://lccn.loc.gov/2020049077
LC ebook record available at https://lccn.loc.gov/2020049078

Published by
SPIE
P.O. Box 10
Bellingham, Washington 98227-0010 USA
Phone: +1 360.676.3290
Fax: +1 360.647.1445
Email: books@spie.org
Web: www.spie.org



Printed in the United States of America.
First Printing.
For updates to this book, visit http://spie.org and type “PM329” in the search field.

# Contents

# Preface to the Second Edition

The first edition of this book was published in 2010. Eleven years is a long time in the field of lithography, even though much of the original content still withstands the passage of time and the advances in the technology nodes. Here are the reasons I decided to update this book:

1. Over these years, I am happy to have fulfilled my original goal of making this book suitable for (1) newcomers to the field who are interesting in growth into a technology career, (2) seasoned professionals who seek more depth into the technology, and (3) managers and executives who seek more breadth. People from each of these groups have told me that the book helped them and that they would recommend it to new readers. With this new edition, I hope to make the book even more useful.
2. For more than three years since my retirement from TSMC in Nov. 2015, I have taught the course Innovative Lithography, using the materials in this book. My students have given me the inspiration and enthusiasm to improve and update the book.
3. Lithography technology is fun to learn, fun to practice, and fun to teach. It is gratifying for me, once again, to preserve this knowledge in a book so that the torch can be passed.

This second edition features the following updates:

Chapter 2 Proximity Printing. This is a completely new chapter. In universities and many research labs, people need to make patterns with less-expensive equipment. Therefore, proximity printing is still very popular, even though there are not many publications on proximity imaging. I show rigorous and approximate ways to simulate the diffracted image at contact and in near, medium, and far fields, as well as the region of validity of these methods. The unintuitive positive- and negative-resist images from the proximity image are plotted. The E-G diagrams (from various authors) for quantifying proximity imaging are also covered. An appendix is provided to document our (two of my graduate students' and my) extensive research on methods to determine the region of validity of the approximation methods studied.

Chapter 3 Exposure Systems. To complement the coverage of historical and current exposure systems for replicating patterns described in the first edition, a carefully prepared step-by-step illustration of the mask and wafer movements in a step-and-scan system has been added. I also clarify that the projection-printed image is a mirror image, despite the common impression that only proximity printing produces a mirror image.

Chapter 4 Image Formation. In addition to adding derivations of the resolution-scaling and DOF-scaling equations and analyses of spatial frequency, light–resist interaction, and resist image development, I almost completely rewrote the section on Zernike polynomials, making their concepts easier for lithography engineers to grasp. The simulated partially coherent images in this chapter have been updated.

Chapter 5 E-D Methodology. This chapter is timeless. I provide a detailed explanation of how to construct E-D trees and emphasize why the log scale is preferred for intensity and exposure. The term apparent exposure —the reciprocal of intensity—is introduced, and its use in E-D diagrams is explained.

Chapter 6 Hardware Components. In this long chapter on lithography components, I added examples of some enlightening resist development phenomena to help people visualize the resist development process. The coverage of chemically amplified resists is expanded. The coverage of wafers, the wafer stage, and alignment systems is also enriched.

Chapter 7 Processing and Optimization. This is another long chapter. I added new insightful derivations of off-axis illumination and a demonstration of extracting the overlay error components with a redundant number of data points to improve the accuracy. Multiple patterning is also extensively discussed, and the G-rule for double patterning is introduced.

Chapter 8 Immersion Lithography. This chapter continues the thorough coverage of this technology from the first edition with an outlook of its extendibility and its impact on the semiconductor technology. The best scaling equations for resolution and DOF are given, and the numerical aperture of the reduction immersion system is clarified.

Chapter 9 EUV Lithography. I almost completely rewrote this chapter, which is quite understandable because of EUVL's rapid growth during the last decade. Given that there are already other books on EUVL, I made sure that my contribution provides a valuable, unique perspective on the technology.

I omitted the material on MEB direct write to leave open the possibility of producing a single volume on this important topic for future development. Finally, I upgraded the figures with color for the eBook. Indeed, all of the figures in the second edition have been modernized.

I credited my wife Sue for her support of the first edition and of my life in general. Before starting my work on this revision, we celebrated our 50th anniversary in 2018. Sue continues to be an indispensable partner for her

support during my writing of this second edition and her support in my professional life, family life, and spiritual life.

**Burn J. Lin**
July 2021

# Chapter 1
# Introduction

Lithography creates a resist image on the wafer. The subsequent etching, lift off, or ion implantation process is masked by the resist image at the areas dictated by the lithography mask. Hence, the thin-film material on the wafer is selectively removed or built up, or its characteristics are selectively altered. The resist image is produced by replicating the mask pattern, except in the cases of mask making or direct writing on the wafer. Figure 1.1 depicts the mask replication process with an imaging lens. Light from the source is collected by the condenser to illuminate the mask pattern. It passes through the imaging lens to form an aerial image that selectively exposes the resist. After development, the resist image as shown is produced. Figure 1.2 illustrates various forms of image transfer from the resist to the underlying thin film. The film can be isotropically or anisotropically etched, lifted off, plated, or implanted, using the patterned resist as the mask. Detailed descriptions of these transfer processes are given in Chapter 4.

The image formation process is facilitated with an information-carrying beam consisting of photons, electrons, or ions. Optical lithography uses photons to carry out this process. Photons with energy ranging from visible to x-ray wavelengths can be used. However, in this book, the wavelengths of consideration are between 157 and 436 nm, as well as 13.5 nm. These wavelengths are already fully employed in manufacturing semiconductor integrated circuits, except for 157 nm, which was forsaken after a lot of heavily invested learning in research and development, and was replaced by 193-nm water immersion, resulting in an equivalent wavelength of 134 nm. More details on 193-nm immersion lithography are given in Chapter 8. Chapter 9 covers the 13.5 nm extreme-UV (EUV) light that has started to be used for manufacturing 7-nm circuits.

The purpose of this book is to present the working principle of each area in optical lithography by providing examples instead of recipes on *how* to do things. This way, readers understand *why* some techniques are used under certain circumstance and why other techniques are not used. The aim is for

# Chapter 2
# Proximity Printing

## 2.1 Introduction

Soon after the integrated circuit (IC) was invented[1] in 1958, lithography was used to replicate the designed pattern on the mask to the wafer. The most intuitive way to do so is to copy the mask pattern by direct contact of the mask and the wafer. No lens is needed, the field size can be as large as the mask, and the wafer does not even need to be precisely focused. This replication technique was called contact printing, but this is a misnomer. Unless a deliberate effort is made to achieve intimate contact, the mask and the wafer contact each other only at a few points over their entire area. Even if intimate contact is achieved, because there is a photoresist layer between the mask and the wafer, the mask is still in proximity to the wafer by the thickness of the photoresist. In reality, intimate contact is not desirable for the following three reasons. (1) When the mask and the wafer are in intimate contact, high-contrast interference fringes will form wherever there are slight imperfections of contact, as shown in Fig. 2.1. These fringes make the contact exposure nonuniform. (2) The mask and the wafer become difficult to separate after intimate contact. (3) Damage to the mask and the wafer is inevitable. Therefore, the proper lensless way to replicate a mask pattern is proximity printing, not contact printing.

The proximity printing system consists of a light source, an illuminator, a mask, a wafer, and a wafer stage that holds the wafer at a fixed distance from the mask, usually by putting spacers on the mask. Either the mask or the wafer is pressed hard against the other, with the spacers in between. The stage also has the means to move the wafer with respect to the mask for alignment purposes; there are alignment-viewing devices to guide lateral positioning on the wafer. A schematic of a proximity printing system is shown in Fig. 2.2. The system consists of illumination from the light source and the condenser. The mask and wafer are held in their respective holders to maintain a distance on the order of 20 μm between the absorber surface of the mask and the resist surface of the wafer. A larger distance prevents damage to the mask and the wafer; however, resolution is reduced rapidly as the mask-to-wafer gap

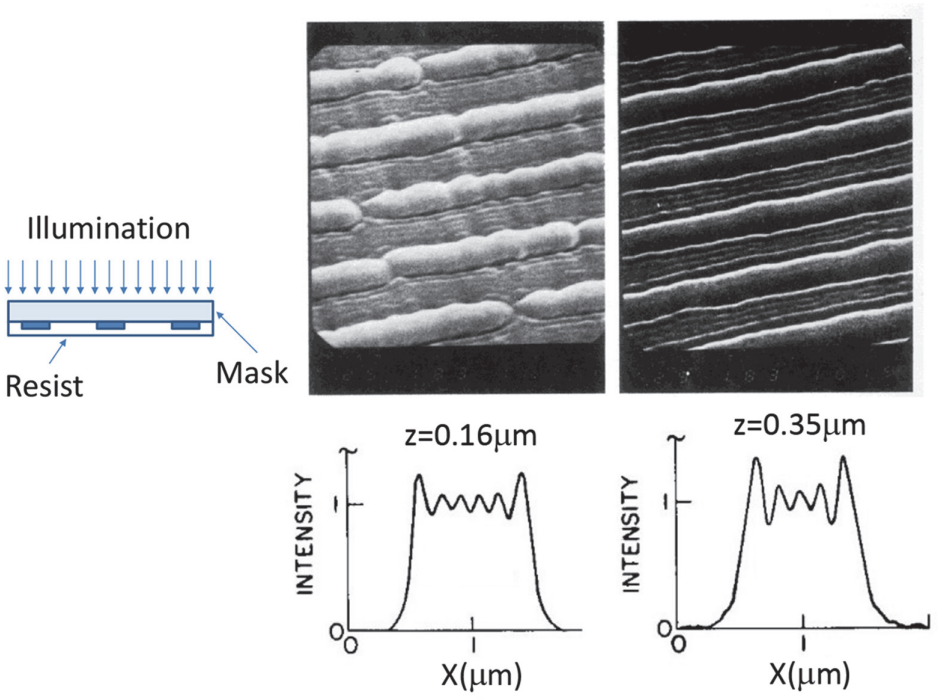


**Figure 2.27** Experimental results of near-field diffraction.

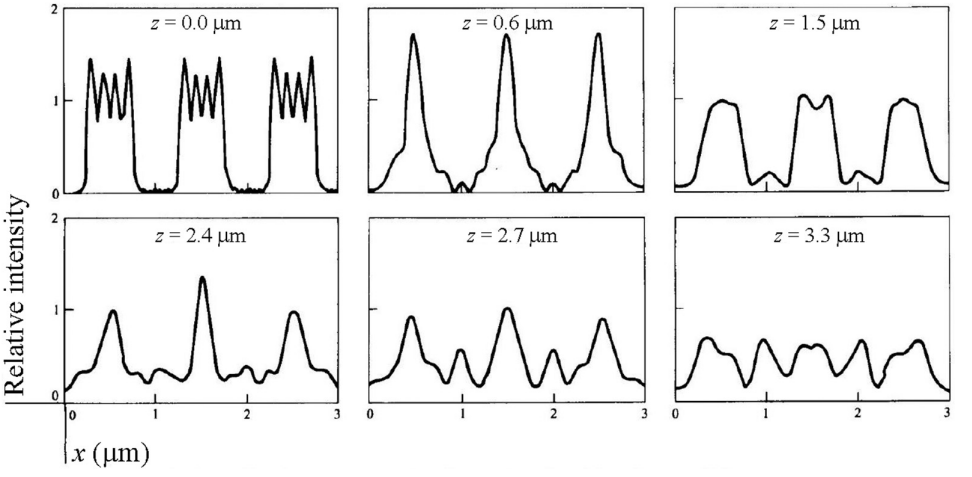


**Figure 2.28** Proximity image in 0-, 0.6-, 1.5-, 2.4-, 2.7-, and 3.3-μm gaps.

intensity distribution has fringes as expected, even though polychromatic illumination is used. At $z$ = 0.6 μm, the image sharpens as it is in focus. It broadens at 1.5 μm and sharpens again at 2.4 μm. At 2.7 μm, the three main

# Chapter 3
# Exposure Systems

Before getting into imaging theory and practice, I would like to present exposure systems so that readers have the right perspective to approach Chapters 4 and 5.

An exposure system reproduces the mask image at the wafer side to expose the photoresist layer on a wafer. The reproduced image can be the same size as the mask image in a 1X system. Reproduction on a modern exposure system usually reduces the reproduced image by a factor of 5 or 4, making it a 5X or 4X system, respectively. After development, this resist image is used as an etch, implant, plating, or lift-off mask for pattern transfer to a thin-film layer on the wafer.

There are different systems for reproduction. When the feature size was in the 2- to 5-μm regime, and the budget for semiconductor manufacturing was low, the aerial image in the 20- to 40-μm proximity of the mask sufficiently produced a useable resist image, maintaining feature size and placement control as covered in Chapter 2.

Below 2 μm, infidelity of the aerial image, defect generation, and alignment viewing difficulties drove the bulk of exposure systems to 1X full-wafer projection printing. The 1X full-wafer coverage fills the requirement of a smooth transition from proximity printing to projection printing.

When the minimum feature size of integrated circuits reached 1 μm, the field size of full-wafer systems grew with the wafer size from 50 to 125 mm in diameter. This ever-increasing wafer size and reduced feature size—together with the associated requirements of feature-size control and overlay accuracy—drove exposure systems to reduction step-and-repeat. Reduction is used to addresses the need to resolve smaller features, tight feature-size control, and overlay accuracy. The step-and-repeat feature is used to accommodate the ever-increasing wafer size in order to overcome the limited image field size of a projection system.

This chapter describes projection-printing systems, 1X and *n*X systems, and full-wafer, step-and-repeat, and step-and-scan systems. The significance of reduction imaging is also analyzed.

# Chapter 4
# Image Formation

As discussed in Chapter 1, the goal of lithography is to place the edges of a given mask pattern on the wafer within a specified tolerance. Doing so with effective controls requires a good understanding of the image formation process—from the mask image to the final transferred image. The aerial image is formed from the light that illuminates the mask and carries the information of the mask pattern through the lens to focus on the image plane. The aerial image becomes reflected and refracted as it propagates into the resist and is reflected and refracted numerous times by the resist, as well as by the multiple film layers on the wafer substrate. The superposition of reflected and refracted images in the resist exposes this medium, producing chemical and physical changes. The distribution of these changes is the latent image. The exposed resist has a distribution of dissolution rate according to the latent image. The developer removes the resist according to the dissolution rate distribution and the topography of the resist surface. The developed resist is now the resist image. The transferred image is dictated by the resist image and the characteristics of the transfer process. These images are discussed below.

## 4.1 The Aerial Image

We define the aerial image as light distribution at the vicinity of the image plane without any resist or multiply reflecting surface. The image must be treated as light waves in physical optics as opposed to light rays in geometric optics. When the light wave has a perfect wavefront to form the image, there is no aberration to deteriorate the image. The only limit on resolution comes from the finite extent of the wavefront dictated by the aperture of the imaging lens. A larger aperture produces a better diffracted image. Such an imaging system is called a diffraction-limited system. We start our investigation using a perfect spherical wavefront with a finite lens aperture to form a point image, which leads to the relationship of diffraction-limited resolution to wavelength and aperture size, followed by the relationship of depth of focus (DOF) to the same set of parameters. Deviation from the spherical wavefront is treated in

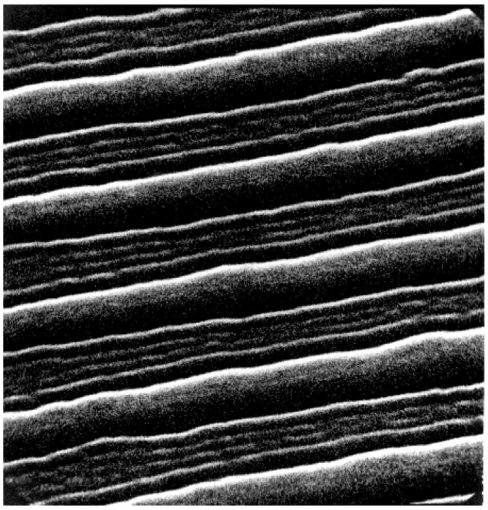

**Figure 4.14** Experimental recording of an exposure intensity (electric field squared) distribution 2.1λ away from a 6.6λ-wide slit.

outside the lens aperture and is unity inside when there is no aberration. Otherwise, $G = 1 + \psi/r$, where $\psi$ and $r$ are defined in Eq. (4.27). The coordinates $(x_o, y_o)$, $(\xi,\eta)$, and $(x_i, y_i)$ are depicted in Fig. 4.15. As mentioned earlier, photoresist responds to light intensity, not the electric field. Once the electric field distribution is determined, the intensity distribution simply follows from this equation:

$$I(x_i, y_i) = E^*(x_i, y_i)E(x_i, y_i). \tag{4.52}$$

#### 4.1.5.2 Incoherent imaging from a mask pattern

With incoherent imaging, the phase relationship between different image points is completely random, as depicted by Fig. 4.16. Although the phase relationship within one infinitesimal object point and its conjugate image point remains deterministic, it is impossible to pinpoint the electric field deterministically. However, the intensity distribution is readily evaluated using

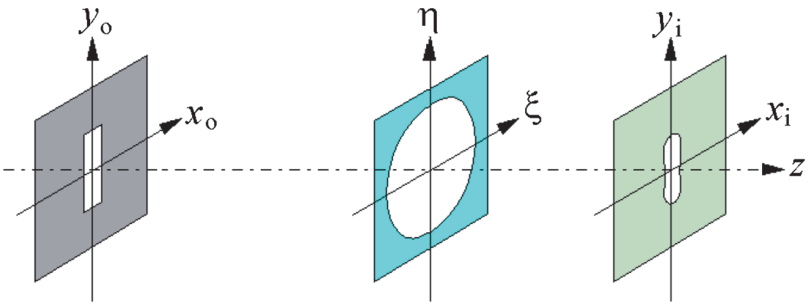


**Figure 4.15** Object, pupil, and image coordinates.

# Chapter 5
# The Metrics of Lithography: Exposure-Defocus (E-D) Tools

In microscopy, one is concerned with the closest distance between two objects that can be resolved in the image. The points of concern are quite different in lithography. A low-contrast image with a shallow intensity slope can be turned into a sharp edge with the photoresist. As mentioned in Section 1.3, the location of this edge is of prime interest and must be quantified against the operating parameters of the exposure tool during manufacturing because it determines the feature size that may be related to circuit switching speed, leakage, resistance, etc. In addition, the edge position also determines whether the image in a given layer can be effectively overlaid with previous or subsequent layers. The five primary parameters that can be adjusted in the field are exposure dosage, focal position, pattern alignment between layers, magnification, and rotation. The last three parameters are mostly related to overlay. Even though magnification can affect feature size in principle, its effect on overlay is much greater than on feature size. The first two parameters, exposure dosage and focal position, determine the process window of the lithographic system in a mutually dependent way. This mutual dependence and the ability to superimpose simultaneous requirements on different features are captured in exposure-defocus (E-D) tools, which are the backbone of lithography metrics.

## 5.1 The Resolution and DOF Scaling Equations

Section 3.2 introduced resolution and DOF scaling in projection printing using the proportional relationship to wavelength and inversely proportional relationship to the lens numerical aperture without introducing the proportional constant. Equations (4.12) and (4.16) used an arbitrary constant 0.5 to provide the physical meaning of these relationships. Here, we finally introduce the resolution and DOF scaling equation with rigorous proportional constants $k_1$ and $k_3$. The reason for the delay in presenting this equation

# Chapter 6
# Hardware Components in Optical Lithography

An optical lithography imaging system includes the following key components: a light source that provides the exposure photons with the desired energy spectrum; an illuminator that collects light from the source, adjusts its coherence and incident angles, and delivers light to the mask uniformly; a mask containing the circuit image to be replicated to the photoresist; an imaging lens of the desired NA and field size to reproduce the mask image in the resist by exposure; the resist layer coated on the wafer; the thin-film stack to be delineated by the pattern-transfer process or implantation; the wafer held by a chuck on a wafer stage that can be moved for alignment and field stepping; and alignment-viewing devices to guide the aligning movement of the stage. These components are described consecutively in the following sections.

## 6.1 Light Sources

There are two types of light sources for use in optical lithography exposure tools: the mercury arc lamp and the excimer laser. These light sources are bright and efficient in their respective wavelength spectra.

### 6.1.1 Mercury arc lamps

The mercury arc lamp has been the light source of choice for optical lithography because of its many usable emission lines in the near-UV(350–460 nm), mid-UV (280–350 nm), and deep-UV (200–280 nm) regions. There is even an emission line at 184 nm. This lamp's high brightness compared with other nonlaser sources is another reason for its popularity. Figure 6.1 shows the radiation spectrum of a typical mercury arc lamp. Figure 6.2 shows a schematic drawing of a mercury arc lamp. Pointed and rounded electrodes are enclosed in a quartz envelope that contains a noble gas and a drop of mercury. During ignition, electric discharge takes place between the two electrodes. As

## 6.2 Illuminator

The illuminator of a typical scanner is shown in Fig. 6.9. The laser beam goes through the beam-pointing-and-steering unit and the variable attenuator to adjust its direction, position, and intensity before entering the illumination shaping optics. There, the beam is shaped for the type of illumination, such as axial, off-axis, Quasar, etc. To reduce the spatial coherence, the beam passes through the quartz rod, where its illumination energy is monitored. The coherence of the illumination is determined at the reticle masking assembly. Together with the imaging lens, these components constitute a Köhler illumination system. At the reticle masking assembly, the area outside of the printed area of the reticle can be masked off.

### 6.2.1 Köhler illumination system

A typical Köhler illumination system[13] is shown in Fig. 6.10. The key to Köhler illumination is that the source plane is conjugate to the pupil planes, which are, of course, conjugate to each other. Hence, the rays originating from the source point $Q_s$ converge at point $Q_{P1}$ at pupil 1. They converge again at $Q_{P2}$. The rays from other source points, represented by the other ray at the reticle opening $A_{M,}$ go through the imaging lens system, including pupil 2, to converge at the wafer at $A_W$. There are now two conjugate relationships, one linking the source plane and pupil planes, and the other linking the reticle plane, wafer plane, and reticle masking plane in the reticle masking assembly.

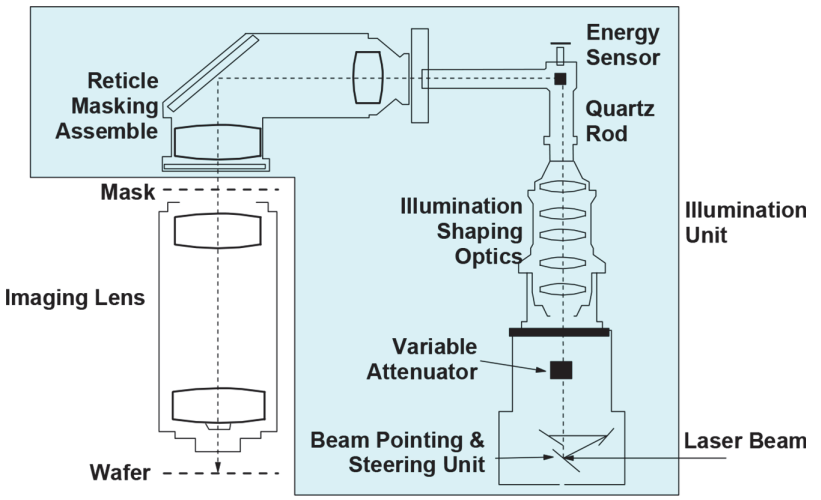


**Figure 6.9** Schematic drawing of the illumination unit of an ASML scanner (reprinted with permission from ASML).

# Chapter 7
# Processing and Optimization

Now that we have provided sufficient background on imaging and tools, the processes that use them and the optimization of these processes are given in this chapter. We start with optimization of the exposure tools, then move on to resist processing, $k_1$ reduction schemes, and finally the control of critical-dimension (CD) uniformity and overlay accuracy.

## 7.1 Optimization of the Exposure Tool

The optimization of an exposure tool involves the optimization of its numerical aperture (NA), illumination setting, exposure/focus, depth-of-focus (DOF) budget, and monitoring of focus, as well as its throughput optimization in field size and exposure routing.

### 7.1.1 Optimization of the NA

Most modern exposure tools and steppers allow users to adjust the NA of the imaging lens because the NA cannot be preset in the factory when the resolution is extended to the low-$k_1$ regime. The optimum NA[1,2] is not the highest one in the range of available settings on the tool, but rather is a function of feature size and shape combinations, illumination, etc. It is important to set the NA to the best value to take advantage of the capability of the imaging system.

From Eq. (5.3), the resolution scaling equation, $\sin\theta$ must be sufficiently large to sustain the resolution of a given feature. However, Eq. (5.4) dictates that a large $\theta$ reduces the DOF. Therefore, in a dry system where the space between the last lens surface and the resist is not immersed in a liquid, the NA of its imaging lens has a medium value whose DOF is maximum. Figure 7.1 shows the DOF as a function of the NA at $\sigma = 0.82$ for 0.20-μm resist lines separated by 0.20-μm spaces. The DOF is evaluated with the exposure-defocus (E-D) forest methodology covered in Chapter 5, based on 8% EL and CD bounds at ±15 nm. The DOF quickly rises from 0 to 1.04 μm at $NA = 0.557$, then gradually decreases as the NA increases. Figure 7.2 depicts

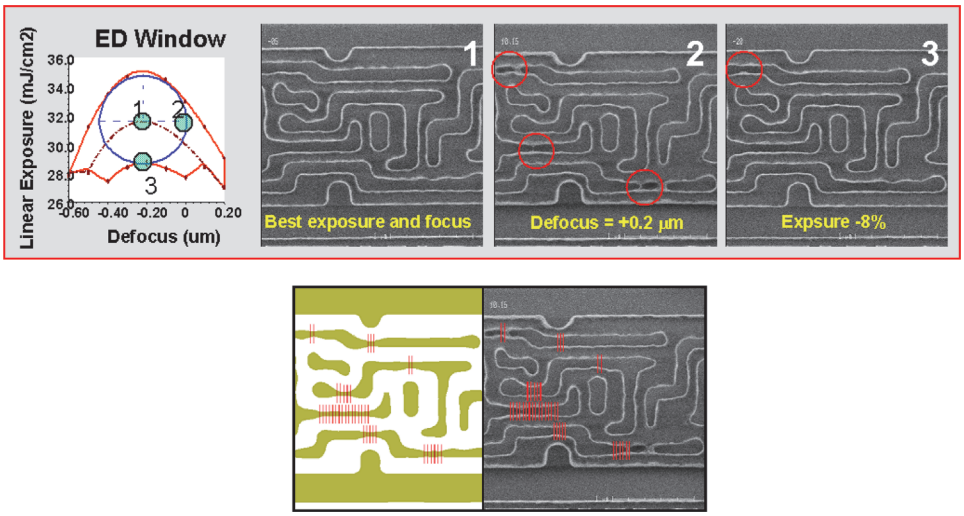


**Figure 7.115** Series of resist images in the top row indicating hot spots near the boundary of defocus and exposure. The markings in the lower row show the detected hot spots on the left and the corresponding locations on the resist image on the right (images courtesy of R.G. Liu).

### 7.3.4.8 Hot-spot checking

After OPC, but before sending the data for mask making, it is preferable to perform a hot-spot check to fine tune the corrected mask pattern. The reason is that the OPC spec is based on the summation of the deviation from the target image at all target points. This addresses the fidelity of a single image edge but not the distance between nearby edges. There may be situations where two edges get too close. Even though the design rule before OPC addresses feature size and the distance between edges on the design, OPC changes them. The optical-proximity-corrected image must be examined. Figure 7.115 shows the formation of hot spots at the boundary of the defocus and exposure. In the lower row, the hot spots identified with a hot-spot check are marked on the optical-proximity-corrected image and the resist image.

## 7.4 Polarized Illumination

As the feature size of integrated circuits shrinks to the subwavelength regime, polarization of the illumination becomes very important. A lot of resolution can be lost with the wrong polarization. Therefore, polarization can be considered as another $k_1$-restoration technique. The logical placement of polarized illumination in this book should be here. However, this topic was extensively explored in the first edition in the chapter on immersion lithography. In order not to drastically disturb the original organization of this book, this discussion and its update remain in Chapter 8.

# Chapter 8
# Immersion Lithography

## 8.1 Introduction

Immersion lithography is a dark horse. The International Technology Roadmap for Semiconductors (ITRS)—documents adopted by all equipment and material suppliers—together with semiconductor manufacturing companies reduced the actinic wavelength from 436 nm to 365 nm, 248 nm, 193 nm, 157 nm, then 13.4 nm. The 436- and 365-nm wavelengths are two prominent lines produced by the mercury arc lamp. The 248-, 193-, and 157-nm wavelengths are generated by XeCl, KrF, and $F_2$ excimer lasers, respectively, followed by 13.4-nm EUV light, initially generated by Xe plasma, and then enhanced by switching to Sn plasma.

The ITRS continued to be followed over the years. Just before the year 2000, 193-nm lithography was projected to reach its limit with the 0.93-NA imaging optics, which can handle the 65-nm node and stretched to the 55-nm half node. However, following the roadmap, the industry started working on developing 157-nm lithography much earlier than year 2000.

Unfortunately, only $CaF_2$ is suitable for lens material at such a short wavelength. This material has been used in 193-nm applications, but the specification is much more stringent for 157 nm. A heavy investment was made to grow a large, perfect $CaF_2$ crystal for the imaging lens, but this attempt was not successful. A major reason for the failure is the 90-day turnaround time required to grow the large crystal. As many as 600 crystal-growing furnaces have been employed to develop the $CaF_2$ production process, but to no avail.

Developing a resist for 157 nm also faced tough challenges. Until the worldwide termination of the 157-nm program, no satisfactory resist had been demonstrated. The pellicle material was also wanting. No suitable membrane material was available. The only option was to use quartz or $CaF_2$ as a thick pellicle. Then, mounting and demounting the pellicle without affecting the optical performance of the imaging system became a difficult problem. Lastly, oxygen absorbs 157-nm light, so the optical path must be in nitrogen, making the system inconvenient and hazardous to operate. Even though nitrogen is

### 8.6.3 The immersion lens

The challenge with immersion lenses varies greatly depending on the required NA. When the NA of a dry system is to be used for immersion, as in the case of Fig. 8.4, it is not difficult to design and fabricate the immersion lens. The major change involved in moving from dry to immersion is the reduction of the working distance to utilize the short optical distance required to minimize the effect of inhomogeneity. However, when $NA > 1$ is needed, the bending angles in the lens are harder to manage.[30,31] At $n_{CM} = 1.44$, the design limit appears to be 1.3 ~ 1.35 NA for some lens designers.[35] Above 1.2 NA, the field size of the conventionally configured lenses may need to be reduced to keep the size of the projection optics within physical and economic viability. It is well known that field size reduction substantially lowers the productivity of the exposure tool. Fortunately, the NAs of modern immersion lenses without a reduction in field size[36,37] are as large as 1.35. These are catadioptric systems, not simply dioptric. It is important that the catadioptric system does not introduce a mirror image of the mask. This can confuse the circuit designer, leading to unnecessary manufacturing errors. Therefore, the number of reflecting surfaces should not be an odd number. Figure 8.44 shows Zeiss high-NA immersion lenses[38] that have been installed in commercial scanners. Figure 8.45 shows four high-NA Nikon lenses[39] that were under development in 2007.

One needs to distinguish between the use of immersion lithography for attaining DOF extremes and for attaining resolution extremes. For the former purpose, immersion lithography extends the life of an existing imaging system to near-term new technology nodes (e.g., from the 65-nm node to the 45-nm

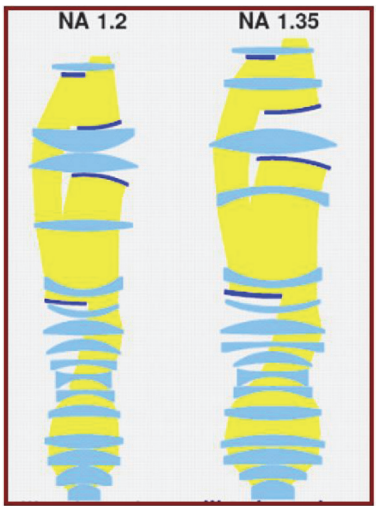


**Figure 8.44** Zeiss high-NA immersion lenses that have been installed in commercial scanners (reprinted from Ref. 38).

# Chapter 9
# EUV Lithography

## 9.1 Introduction

Optical lithography in the regime of $k_1 = 0.28$ is very complicated. The image contrast is low and, except for 1D single-pitch patterns with special illuminations, the mask error enhancement factor (MEEF) is high. For contact hole patterning, the MEEF can be more than 4, which negates the gain of a 4X reduction system. Line ends can have MEEF as high as 10. In addition, the shape of patterns at low $k_1$ is rounded out and requires a significant amount of optical proximity correction to keep the patterns usable. Extreme-UV lithography[1,2] (EUVL) previously used the 13.4-nm wavelength. Recently, this technology migrated to 13.5 nm. Either wavelength offers an order of magnitude reduction in wavelength from the water-immersion ArF wavelength of 134 nm. This presents an opportunity to bring $k_1$ back to above 0.5. It is no wonder that EUV lithography has attracted large research and development efforts worldwide. The size of the EUV development effort has dwarfed two other well-known lithography developments, namely, 157-nm lithography and x-ray proximity printing. Take the 32-nm half pitch. At the water-immersion ArF wavelength of 134 nm and $\sin\theta = 0.95$, $k_1$ is 0.227. Turning to EUV at $\sin\theta = 0.25$, $k_1$ becomes 0.597. Initially, the term soft x-ray[3] was used to identify this lithography. However, the use of UV light has had an impressive history of success compared to x-ray lithography. It makes sense to associate the technology with the winning wavelength range, thus it is called EUV lithography. Since the publication of Ref. 1 in 1989, more than three decades have passed and many challenges have been met. EUVL for production of the 7-nm node has been demonstrated.[4] High-volume manufacturing is expected to follow. It will be worthwhile to track the number of nodes by which the three decades of development efforts can extend semiconductor scaling.

With such a dramatic drop in wavelength, the imaging system is substantially different from existing systems. First, EUV light is heavily absorbed by any substance, including gases. The optical path must be in vacuum. Second, because of EUV light's strong absorption characteristics, there is no transmitting material—EUV optical imaging depends on reflection.

slot field is taken from a large circular field, as in a scanner lens. The image quality should be uniformly good. Even after taking aberrations into consideration, the uniformity of the imaging quality of such a slot field should still be much better than that from a slit field.*

The illuminator used in the ASML EUV alpha tool is shown in Fig. 9.5. The collector reflects the EUV light at the IF such that the light goes through the illuminator optics (consisting of two normal-incidence mirrors and two grazing-incidence mirrors) to reach the mask. This simplified illuminator is used here to show a typical number of mirrors in an illumination system. Production-type illuminators that need to enable OAI, source optimization, and source mask optimization, as well as to control the partial coherence, are much more complicated, just like the DUV illuminator. Examples of some illuminators can be found in Section 5.5.3 of Ref. 19.

## 9.2 EUV Source

The EUV source has been a key bottleneck of EUVL for high-volume manufacturing; the power level has been insufficient to support a viable throughput. After an enormous investment of billions of dollars by suppliers and potential users that involved the research of thousands of individuals, engineering prowess combining talents in many disciplines, management and marketing skills, will power, and vision, the EUV source can now support an acceptable but not exciting throughput. The path to further increasing the source power is now visible, but this high power brings additional challenging problems concerning power grid loading, heat removal, and environmental impact. Before discussing the working principle of the source, let's first consider the source power requirements and impacts. Because there is no optical layout of the illuminator, we use the number of collectors and mirrors in the illumination module of the alpha tool.[54]

### 9.2.1 Source power requirement

An EUV scanner needs to be economical for manufacturing semiconductors. It is anticipated that the scanner itself will cost many times more than a 193-nm immersion scanner. The space required for the EUV source is also many times larger. The raw power required and the consumables such as water and gases are in much larger quantities. Therefore, to avoid cost escalation, it is very important to make the throughput of EUV scanners much higher than that of conventional scanners. This means economically increasing the source power and transmission of the optical system, overcoming the limits in scan speeds, or increasing the resist sensitivity.

*In a step-and-scan exposure tool, we use "slit" to denote a curved field and "slot" for a straight field.

**Burn J. Lin** is a Distinguished Research Chair Professor at the National Tsing Hua University in Taiwan and the Director of the Tsing Hua-TSMC Joint Research Center. From 2011 to 2015 he was Vice President and a Distinguished Fellow at TSMC, Ltd., which he joined in 2000 as a Senior Director. Earlier he held various technical and managerial positions at IBM in the U.S., after joining the IBM T.J. Watson Research Center in 1970. He has been extending the limit of optical lithography for half a century. In 1991, he founded Linnovation, Inc. and is still the CEO of the company.

Dr. Lin is the inaugurating Editor in Chief of the *Journal of Micro/Nanolithography, MEMS, and MOEMS*, a life member of the U.S. National Academy of Engineering, Academician of Academia Sinica, Laureate of the Industrial Technology Research Institute in Taiwan, IEEE and SPIE Life Fellow, and a joint distinguished professor at the National Chiao Tung University and the National Taiwan University. He is also Distinguished Alumni of the Ohio State University and the National Taiwan University.

Dr. Lin is the recipient of the 2018 Future Science Prize in Mathematics and Computer Science, a 2017 SPIE Award for inaugurating the Optical Microlithography Conference in 1987, the 2013 IEEE Jun-Ichi Nishizawa Medal, the first Semi IC Outstanding Achievement Award in 2010, the 2009 IEEE Cledo Brunetti Award, the 2009 Benjamin G. Lamme Meritorious Achievement Medal, the 2007 Industrial Technology Advancement Award, the 2006 Distinguished Optical Engineering Award from the Optical Engineering Society of R.O.C., the 2005 Most Valuable Player in VLSI Research Inc.'s All-Stars of the Chip Making Industry, the 2005 Two Best R&D Managers in Taiwan, the 2004 Outstanding Research Award from PWY Foundation, the first SPIE Fritz Zernike Award in 2004, the 2003 Outstanding Scientific and Technological Worker Award, and the 2002 Ten Best Engineers in Taiwan award. Throughout his career, he has received 2 TSMC Innovation Awards, 10 IBM Invention Awards, and an IBM Outstanding Technical Contribution Award.

Dr. Lin has been pioneering deep-UV lithography since 1975, multilayer resist systems since 1979, simulation of 2D partially coherent imaging since 1980, exposure-defocus methodology since 1980, scaling equations of resolution and depth of focus since 1986, $k_1$ reduction since 1987, proofs of 1X mask limitations since 1987, vibration in optical imaging since 1989, electrical measurement of contact holes since 1989, E-G tree for x-ray proximity printing since 1990, experimental demonstration of the impact of mask reflectivity on imaging since 1990, optimum lens NA since 1990, attenuated phase-shifting mask since 1991, signamization since 1996, LWD-$\eta$ and LWD-$\beta$ since 1999, nonparaxial scaling equations of resolution and depth of focus since 2000, 193-nm immersion lithography since 2002, and

polarization-induced stray light since 2004. His innovations and research efforts have spanned 21 lithography generations, starting at the 5000-nm node and extending to the 5-nm node.

Dr. Lin has written 2 books, 3 book chapters, and more than 132 articles, 71 of which he is the sole or the first author. He also holds 88 U.S. patents.